Design of Hydrogen Supply Networks for Aviation: Dynamic Optimization Model and Transition Pathways for German Airports

Akin Ögrük[1] (ORCID: 0000-0002-7283-6574), Finn Schenke[2] (ORCID: 0000-0003-4319-9753), Richard Hanke-Rauschenbach[2] (ORCID: 0000-0002-1958-307X), Christian Thies[1] (ORCID: 0000-0001-5690-7582)

[1]Hamburg University of Technology, Resilient and Sustainable Operations and Supply Chain Management Group, Hamburg, Germany
[2]Leibniz University Hannover, Institute of Electric Power Systems, Hannover, Germany

Abstract. Hydrogen-based propulsion concepts for aircraft are considered a promising technology towards the decarbonization of aviation. While the development of respective aircraft models is in progress, questions regarding the supply network of green hydrogen are arising. We present a multi-period mixed-integer programming model for the hydrogen supply chain network design problem focusing on the aviation sector. The model minimizes the total network cost by making strategic decisions (e.g. suppliers, locations, capacities, transportation infrastructure) and tactical decisions (e.g. hydrogen flows, storage quantities) at different temporal resolutions. Our model formulation considers the spatially and temporally varying supply and demand of hydrogen, the techno-economic characteristics of hydrogen storage, liquefaction and transportation (e.g., economies of scale), as well as the specific requirements of hydrogen handling (e.g., losses). Model application is illustrated for a representative set of German airports with local production and hydrogen import options, considering the projected development of the European Hydrogen Backbone pipeline infrastructure. Optimal network designs (from production to the airport storage tanks) and corresponding costs are analyzed for different hydrogen demand scenarios. In addition to the model results, refueling costs at each airport are calculated separately, thereby covering the entire end-to-end supply chain and enabling the estimation of hydrogen cost at the pump.

Keywords: Supply Chain Network Design · MIP · Sustainability · Hydrogen (H_2) · Aviation

1 Introduction

The aviation sector accounted for approximately 0.8 gigatonnes (Gt) of global carbon dioxide (CO_2) emissions in 2022, representing 2% of total anthropogenic CO_2 emissions (IEA 2023). Even with projected efficiency improvements in aircraft technology and operations, CO_2 emissions are expected to rise to around 1.9 Gt in 2050 due to the increasing demand for flights (Figure 1). In addition to CO_2, aviation significantly contributes to non-CO_2 climate effects such as contrails and nitrogen oxides, resulting in an overall climate impact estimated at approximately 3.5% of global radiative forcing in 2011 (Lee et al. 2021). This contradicts the aviation industry's target to achieve net zero CO_2 emissions in flight operations (IATA 2023).

One promising strategy to achieve aviation's ambitions CO_2 targets is the development of new aircraft propulsion technology based on alternative fuels. For example, green hydrogen (H_2) could reduce CO_2 emissions of flight operations by 100% and overall climate impact (including CO_2 and non-CO_2 emissions) by 90% (McKinsey & Company 2020). Therefore, it is considered by both academia and industry as one of the most important energy carriers for future aviation. Next to its direct use in aircraft (the concern of this study) it can also serve as a feedstock for the synthesis of sustainable aviation fuels (Hoelzen et al. 2022; Hydrogen Central 2022; IATA 2023).

Academia and industry are working towards the future widespread use of H_2-fueled aircraft. First flights of H_2-fueled aircraft with 40 passengers and up to 1600 km range have already been demonstrated (Rosalyne 2023). Furthermore, Airbus aims to introduce the first commercial H_2-fueled aircraft by 2040 to 2045 (Harrington 2023). With the market deployment of H_2-fueled aircraft, aviation's need for H_2 will increase to significant levels. While global green H_2 production totaled 1.2 Mt in 2021, the green H_2 demand of the aviation sector alone is projected to range between 20 Mt and 42 Mt in 2050 according to IATA (2023) and McKinsey & Company (2020). This projected rapid increase in green H_2 demand requires the development of an effective supply infrastructure.

One major challenge in making green H_2 a viable alternative to conventional aviation fuels is to reduce its cost. Hence, cost-effective end-to-end hydrogen supply chain network design (HSCND) has become an important research focus. However, as the hydrogen market is currently in its nascent stage, researchers and industry are facing numerous challenges and uncertainties in developing efficient HSCND. Key obstacles include demand and supply-side uncertainties, the lack of reliable techno-economic data, and the complexity associated with repurposing existing infrastructure for hydrogen use. Additionally, capacity limitations, the selection of transportation modes, and the strategic planning required to transition the hydrogen supply chain network from its

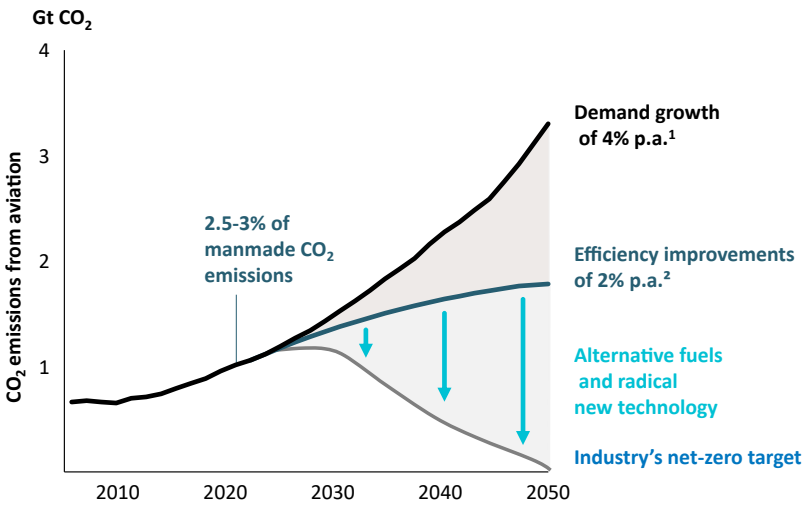

Fig. 1: Projection of CO_2 emission for aviation (Fuel Cells and Hydrogen 2 Joint Undertaking 2020).

infancy to a mature state remain significant hurdles. Addressing these challenges, this study aims to develop a planning model that supports the optimal HSCND across a specified geography and time horizon.

The remainder of this paper is organized as follows. Section 2 examines the problem characteristics and model requirements, which are compared against extant planning models in the literature. Addressing the unique requirements of hydrogen supply chain network (HSCN) for aviation, a mathematical optimization model that minimizes total network cost is developed in Section 3. The application of the model is demonstrated through a case study on green H_2 supply networks for German airports. Section 4 introduces the case study setting, assumptions, and data. Section 5 presents and discusses the results for the different scenarios, while Section 6 provides insights for decision-makers and concludes with potential future research directions.

2 Planning problem

In the following, the characteristics of supply chains of green H_2 for aviation are described. Then, the requirements that must be fulfilled by a planning approach for the HSCND are derived and existing models in the literature are analyzed in terms of these requirements. Finally, the intended contribution of the study is explained.

2.1 Green hydrogen supply chain for aviation

There are various types of H_2, often distinguished by "colors" (e.g., green, blue, pink, gray, etc.), each produced through different methods that carry distinct ecological and economic impacts (Ajanovic et al. 2022). This study focuses exclusively on green H_2. The green H_2 supply chain for aviation consists primarily of the following stages: production of gaseous hydrogen (GH_2), liquefaction, storage, and transportation. Green GH_2 is produced through the electrolysis of water, using electricity from renewable energy sources such as solar and wind (Hoelzen et al. 2022). For aviation, unlike many other sectors, H_2 is required in liquid form due to the low energy density of its gaseous state, necessitating liquefaction to avoid excessively large fuel tanks on the aircraft. GH_2 is stored in pressurized tanks or natural underground storage areas, while cryogenic tanks are required to maintain liquid hydrogen (LH_2) at temperatures below -253 °C. All material flows between the stages of the hydrogen supply chain necessitate transportation. For GH_2, economically and technologically viable transportation modes include pipelines as well as trucks and railway vessels. In the case of liquid hydrogen LH_2, cryogenic truck tanks and sea-going vessels are the primary transportation modes. The generic structure of the green H_2 supply chain is illustrated in Figure 2.

2.2 Problem requirements and analyzing them through existing literature

The problem of designing efficient hydrogen supply chain is closely related to the general supply chain network design (SCND) (Melo et al 2009; Goetschalckx 2011). This problem usually comprises decisions regarding the selection of suppliers, the locations of facilities, the flow of goods through the network, the choice of transportation

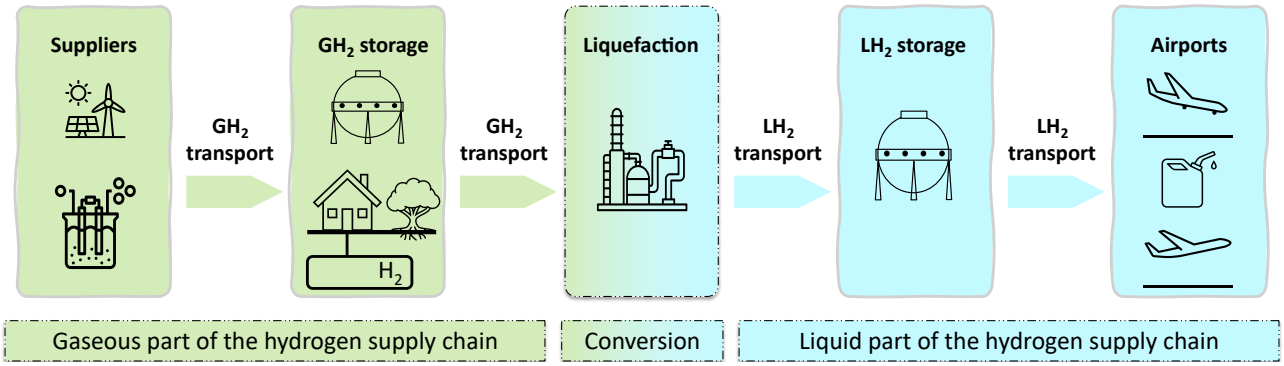

Fig. 2: Generic structure of the green H_2 supply chain for aviation

modes and capacities. In the domain of hydrogen supply chains, there are numerous specific requirements, that are typically not considered by general SCND formulations. These requirements are discussed in the following along with related literature that already addresses them at least partially.

(1) Multi-period models: Long-term planning is essential for an efficient HSCND due to the dynamic nature of pipeline infrastructure, renewable energy capacity, and demand over time. Strategic supply chain decisions, such as determining optimal locations, capacities, and infrastructure investments, carry long-term implications. Thus, instead of employing a static model that captures only a single point in time, adopting a multi-period (dynamic) modeling approach to analyze the network's evolution across interconnected years provides more comprehensive insights and yields more reliable results. While some previous studies (Almansoori et al. 2016; Ochoa-Bique at al. 2018; Ögrük et al. 2025; Reus et al. 2019) focuses on a single period, other studies such as Erdogan et al. 2023, Robles et al. 2019, (Silva et al. 2022), and Yoon et al. 2022) investigate the evolution of the network in a multi-period setting.

(2) Monthly temporal resolution: Green H_2 supply chains must address temporal mismatches between demand and supply, which arise due to the variability of renewable energy sources and fluctuations in aviation demand, particularly during peak periods such as holiday months and other high-travel seasons. Consequently, it is important to incorporate a suitable temporal resolution to account for these fluctuations more accurately. A monthly resolution framework allows for tracking variations in green H_2 production, transportation, and storage quantities on a month-to-month basis, without increasing the model's complexity to the levels required by daily, or weekly resolutions and without oversimplifying operational details as seen in seasonal or yearly resolutions. However, due to the data availability and model limitations, most papers in the HSCN literature adopt annual or even lower temporal resolutions, such as Forghani et al. (2023) and Güler et al (2021). While some studies, such as Reus et al. (2017) and Reus et al. (2019), investigate H_2 storage with seasonal resolution, they do not approach the problem from a complex network perspective where network optimization models are applied. Although not in the H_2 domain, Wolff et al. (2023) optimizes renewable fuel supply chain networks by making tactical decisions with seasonal temporal resolution.

(3) Multi-commodity network flow: Since aviation's H_2 demand is in the form of LH_2, but GH_2 is produced through electrolysis, the supply chain for aviation must handle two distinct H_2 forms. Some studies focusing on other sectors only consider GH_2 (Mukherjee et al. 2015; Raaesi et al. 2024), while others, such as Eskandari et al. (2024), model both GH_2 and LH_2 across the network. Notably, in the aviation context, liquefaction can take place not only at the production nodes but also at the airports, adding additional conversion steps and decisions into the network design. Therefore, multi-commodity flow models must capture both the transport and conversion of H_2 between its gaseous and liquid phases, along with their infrastructure requirements.

(4) Consideration of losses in arcs and nodes: Each H_2 form is associated with distinct losses that arise throughout the transportation, storage, and conversion stages of the supply chain. LH_2 systems experience boil-off losses due to the evaporation of liquid hydrogen under cryogenic conditions. In contrast, GH_2 systems encounter leakage losses resulting from compression, pipeline transport, or handling under high pressure. The type and magnitude of these losses depend on the specific transportation modes, storage technologies, and conversion processes employed across the network. As a result, decisions regarding transport modes, storage capacity, and liquefaction locations must account for these form-dependent losses to ensure efficient and realistic supply chain planning for aviation. Accurately modeling these losses is essential to optimize network performance and minimize hydrogen waste. We observe in the literature that some

studies, such as Fazli-Khalaf et al. (2020), neglect hydrogen losses in their network design, whereas others, like Sizaire et al. (2024), explicitly account for these losses throughout the supply chain.
(5) Multi-modal transportation: Addressing spatial disparities between supply and demand and ensuring access to low-cost H_2 requires the transportation of H_2. Depending on the transported volume, H_2 form and distance, different transportation modes such as trucks, railways, vessels, and pipelines may offer advantages over one another. Therefore, incorporating multiple transportation modes into the network design can significantly influence both its cost-effectiveness and operational performance. Some studies enable only limited transportation modes, such as trucks (De-León Almaraz et al. 2014; Eskandari et al. 2024; Lahnaoui et al. 2021), pipelines (Sens et al 2022; Sizaire et al. 2024) or sea vessels (Kim et al. 2024). However, the literature also includes analyses of models employing multiple transportation modes. For example, Almansoori et al. (2012), Güler et al. (2021) utilize trucks and rail tank cars, while Ohmstede et al. (2023), Ögrük et al. (2025) use both trucks and pipelines.
(6) Utilization of existing infrastructure: Hydrogen is envisioned not only as an energy carrier for aviation but also for numerous other sectors. Consequently, shared infrastructure serving multiple sectors is being planned, offering both economic and operational advantages compared to developing sector-exclusive systems. Given the substantial investments required to establish common H_2 infrastructure and aviation's relatively modest share of its use, allocating only the proportional costs to the aviation sector represents a more efficient and justified investment strategy. According to Cerniauskas et al. (2020), utilizing existing infrastructure allows for a more realistic and cost-optimal HSCND. To this end, incorporating both current and planned pipeline networks, as well as underground GH_2 storage facilities, is a critical requirement in designing the network. In many studies, existing infrastructure is not taken into consideration. For example, Sens et al. (2022) and Wickham et al. (2021) plan the installation of new pipelines between supply and demand nodes without accounting for the use of existing pipelines. The literature contains only a few studies that leverage current or projected infrastructure. For instance, Baufumé et al. (2013) examine the development of a GH_2 pipeline network in Germany to meet future road transportation demand, using existing fuel stations as sink nodes for H_2 demand. Mukherjee et al. (2015) propose utilizing surplus power to produce H_2 for energy storage and distribution, integrating existing natural gas distribution and storage infrastructure. Yoon et al. (2022) utilize byproduct H_2 and existing natural gas pipelines for distribution, finding that using existing pipelines significantly reduces the levelized cost of H_2 compared to non-utilization scenarios. Although not focused on H_2, Uster et al. (2014) optimize Turkey's natural gas network by leveraging and expanding the existing natural gas pipeline infrastructure.
(7) Economies of scale and learnig rate: Capital expenditures ($CapEx$) and operational expenditures ($OpEx$) across different stages of the H_2 supply chain are time- and size-dependent. This variation should be included in the calculations if the model is multi-period or if different sizes of facilities or transportation are needed. Hoelzen et al. (2023) present time-varying techno-economic data for H_2 supply chains using the learning rate method. Almansoori et al. (2009) employ the learning rate concept to calculate costs realistically in their multi-period supply chain design. To cover the size-varying cost data, multiple capacity levels, each associated with distinct unit costs that reflect differences in scale, are utilized. This approach carefully addresses economies of scale, a factor also covered in the literature. Almansoori et al. (2009) and Moreno-Benito et al. (2017) consider economies of scale across various stages of the supply chain, while Forghani et al. (2023) differentiates unit costs for different scales in production and storage facilities but not for pipelines.

While these individual requirements have been addressed separately across various studies, to the best of our knowledge, no existing HSCND model simultaneously integrates all of them. Addressing these interconnected aspects thus necessitates the development of a new, comprehensive modeling framework.

2.3 Approach and intended contribution

To analyze the long-term design and operation of the HSCN, considering monthly green H_2 production potential and demand fluctuations, we formulate a mathematical optimization model. This model integrates multi-period strategic decisions alongside monthly operational decisions. The strategic decisions include capital investment choices regarding the establishment of pipelines and facilities with specific capacities and locations. Meanwhile, operational decisions encompass H_2 flow and storage quantities. The multi-period model incorporates both GH_2 and LH_2 forms, utilizes multiple transportation modes, and, considers economies of scale in both facility and transportation options. Additionally, the integration of existing and projected infrastructure is included into our approach—a dimension that has received minimal attention in the current literature. By incorporating current and future pipeline networks as well as underground H_2 storage facilities along with new capital investments, our approach provides a more realistic foundation for network design. These elements constitute the primary contribution of this study.

Although there is a substantial body of research on hydrogen supply chains and networks, very few studies specifically address these issues within the aviation sector (Hoelzen et al. 2023; Ohmstede et al. 2023). Furthermore, the aviation-focused studies in the literature do not approach hydrogen supply chains from a network perspective. One of the key novelties of this study is that it optimizes the network design specifically for the aviation industry. A distinguishing feature of aviation, compared to other sectors, is that its final H_2 demand is LH_2. This requirement introduces unique supply chain considerations and decisions. For instance, in many HSCND studies for transportation and chemical sectors, LH_2 may be present along the network; however, liquefaction usually occurs at the production site when transport modes such as trucks or sea vessels are required, and LH_2 is subsequently transported and then reconverted to GH_2 at the demand point. In contrast, for aviation, liquefaction may take place either at the production site or at the airport, making liquefaction a critical stage. This flexibility in liquefaction location introduces an additional decision point in the network design process.

To the best of our knowledge, Ögrük et al. (2025) was the first to address these innovations in the context of HSCND for aviation. In the current study, we extend that work by advancing the single-period model to a multi-period framework with a monthly temporal resolution. Additionally, we integrate the possibility of underground GH_2 storage into the framework of existing infrastructure utilization. Based on our literature review, which focuses on the requirements detailed in Section 2.2, we are not aware of any other study that combines all these elements into a single, comprehensive framework.

3 Methodology

In this section, we present our modeling approaches for HSCND and refueling calculations. To determine cost-optimal HSCNs, we first introduce a network optimization model. This is followed by the refueling calculation approach. Due to the deterministic and detailed nature of the refueling process, and the lack of direct interdependency between HSCND and refueling, we treat these two components separately. The network optimization model covers the supply chain from the hydrogen supplier to the airport LH_2 storage tanks (Section 3.1), while the refueling calculations focus on the flow from the LH_2 storage tanks to the aircraft tanks (Section 3.2).

3.1 Network optimization model

3.1.1 Modeling approach

The network optimization model, which is comprehensive extension of the model in Ögrük et al. (2025), combines network design, and the distribution of H_2. The model's underlying network is represented by a directed graph $G = (V, A)$ where $V = D \cup S \cup W \cup L \cup J$ comprises the following nodes: D (demand nodes i.e., airports), S (source nodes i.e., H_2 suppliers), W (comprising underground GH_2 storages (W_g) and LH_2 storages at the airports (W_l)), L (liquefaction nodes), J (junction nodes; consisting of closest connection points on the existing pipeline to the airports, suppliers and underground storages). The set A denotes directed arcs, which define the connections between nodes. Figure 3 illustrates a reduced network for a single supplier - single airport setup.

Each facility in the network is a node $v \in V$ with capacity level $c \in C_v$. Each directed edge $a \in A$, referred to as an arc, connects an origin node v to a destination node $v^{'}$ via a specified transportation mode m, represented as $(v) \xrightarrow{m} (v^{'})$. Thus, an arc a is formally defined as $a = (v, v^{'}, m)$ but for the sake of simple notation, it is referred as a in the rest of the paper. Some of the connections are bidirectional that means if an arc $a = (v, v^{'}, m)$ exists then reverse arc $a^R = (v^{'}, v, m)$ also exists. The time index $t \in T$ is for operational periods and $t^{'} \in T'$ for strategic periods. While operational periods provide the time structure for operational decisions such as flow and storage amounts across the network, strategic periods are realized every n operational periods and used for high-level investment decisions such as the installation or expansion of pipelines, truck fleets, liquefaction plants, and storage facilities (see Figure 4).

The decision variables $x_{v,c,t'} \in \mathbb{Z}_{\geq 0}$ indicate the number of the facilities are deployed at node $v \in V$ with capacity level $c \in C_v$ during the strategic period $t^{'} \in T^{'}$. It is assumed that once a facility is activated in period t', it remains operational until the end of the modeling period, as facility lifetimes exceed the modeled period. The quantity of transportation equipment deployed on each arc is represented by the variable $y_{a,c^{'},t'} \in \mathbb{Z}_{\geq 0}$, defining the configuration of an arc with different capacity levels $c^{'} \in C_a$ for strategic time periods $t' \in T'$. Similar to facilities, once an arc is activated with the specified capacity level, it remains active till the end of the modeling period.

The clear separation of gaseous and liquid network components allows the use of a single-commodity flow $h_{a,c^{'},t} \in \mathbb{R}_{\geq 0}$ which represents the amount of either GH_2 or LH_2 initially entering an arc. We also differentiate

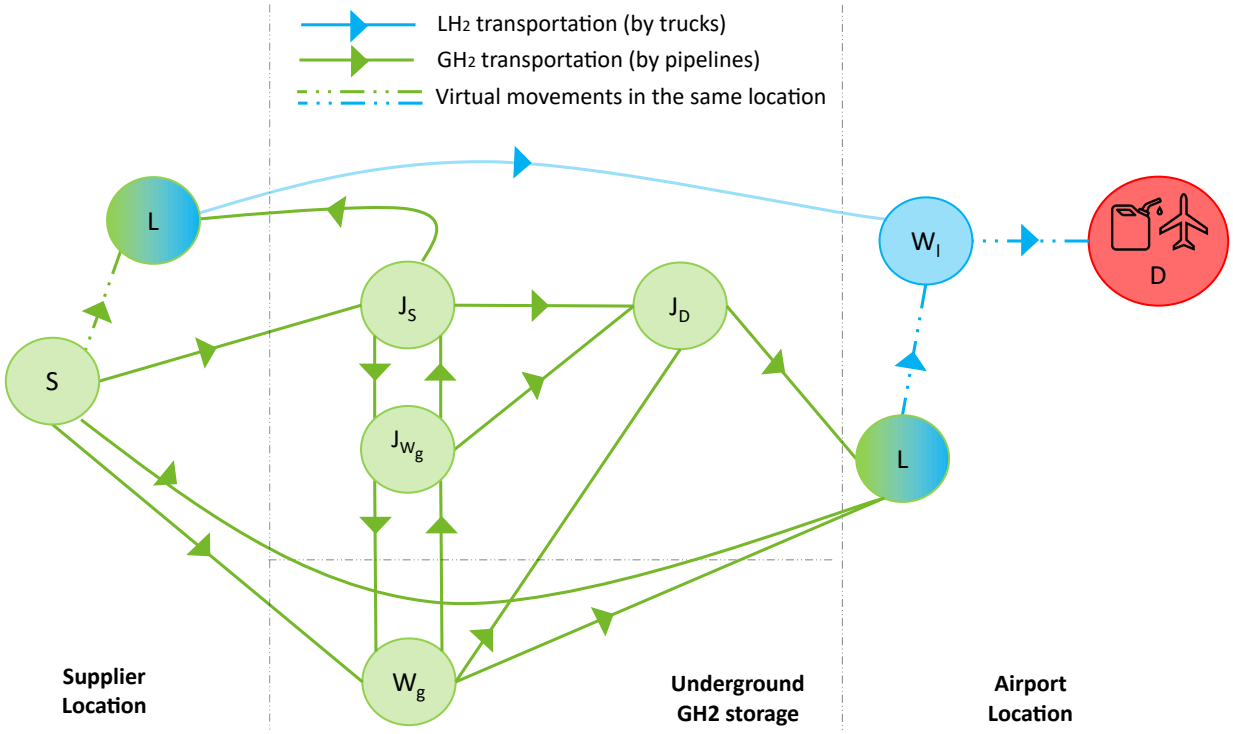

Fig. 3: Reduced superstructure of the HSCN

Strategic periods $t' \in T'$	$t' = 1$			$t' = 2$			...	
Operational periods $t \in T$	1	...	n	$n+1$	...	$2n$	$2n+1$	...

Fig. 4: Representation of operational and strategic time periods

the throughput at the nodes based on capacity levels to account for varying cost factors across different capacity levels. To achieve this, we define the decision variable $g_{v,c,t} \in \mathbb{R}_{\geq 0}$ which represents the amount of H_2 entering the different capacity levels (facilities) of the nodes. Besides, $s_{v,c,t} \in \mathbb{R}_{\geq 0}$ stands for the amount of stored H_2 in W_g nodes while storage in W_l is determined exogenously and not a model variable.

Each facility is associated with the following attributes: node capacity $b_{v,c}$, CapEx (capital expenditure) $k^{\text{CapEx}}_{v,c,t'}$, OpEx (operating expenditure depending on the hydrogen throughput) $k^{\text{OpEx}}_{v,c,t}$, and maintenance cost $k^{\text{O\&M}}_{v,c,t'}$ (which includes costs such as maintenance, insurance, etc. that only depends on capacity but not on throughput). Each arc configuration provides a capacity $b_{a,c'}$, capital expenditure $k^{\text{CapEx}}_{a,c',t'}$, operating expenditure $k^{\text{OpEx}}_{a,c',t}$, and operations and maintenance expenditure $k^{\text{O\&M}}_{a,c',t'}$. All parameters belong to $\mathbb{R}_{\geq 0}$. The detailed lists of decision variables and parameters are given below.

Since the modeling period is shorter than the lifetime of the facilities and arcs, CapEx has to be reflected accordingly. For this, we incorporate the annuity cost factor (ACF) into our cost calculations to accurately reflect the cost share of each CapEx. The ACF is multiplied by the total investment, and the resulting value is allocated to each year from the investment period until the end of the modeling horizon. This approach is widely adopted in the literature (Almansoori et al. 2016; Sens et al. 2022). The ACF represented by ϕ , ranging from $[0, 1]$, is calculated for both arcs and nodes as follows:

$$\phi = \frac{\mu(1+\mu)^{\gamma}}{(1+\mu)^{\gamma} - 1} \tag{1}$$

where γ is the depreciation time, and μ denotes the weighted average capital cost (WACC) for the capital investment. Accordingly, the WACC can be defined as:

(2) $\mu = \alpha^{debt}(1-\omega)\rho^{debt} + \alpha^{equity}\rho^{equity}$

where α^{debt} and α^{equity} denote the debt and equity shares over the initial capital expenditures; ρ^{debt} and ρ^{equity} are the annual rates of return on debt and equity; whereas ω represents the corporate tax rate.

3.1.2 Model notation

Sets

$G = (V, A)$	Model's underlying network.
V	Set of all nodes of the network where $V = D \cup S \cup W \cup L \cup J$ and ; $v \in V$
A	Set of directed arcs, which define the connections between nodes; $a \in A$ where a consists of $(v, v^{'}, m)$ i.e. from node v, to node $v^{'}$, by transportation mode m
D	Set of airports (demand) nodes
S	Set of supplier (source) nodes e.g., production hubs
W	Union of underground GH_2 (W_g) storage and airport LH_2 (W_l) storage tank nodes
L	Set of liquefaction nodes
J	Set of junction nodes
C_v, C_a	Set of capacity levels for nodes and arcs respectively; $c \in C_v$, $c^{'} \in C_a$
M	Set of transportation modes; $m \in M$
T, $T^{'}$	Set of operational and strategic periods respectively; $t \in T$, $t^{'} \in T^{'}$ where $T' \subseteq T$

Decision variables

$x_{vct'}$	Integer decision variable indicating the number of facilities deployed at node v, with capacity level c, during strategic period t'
$y_{ac't'}$	Integer decision variable indicating the number of transportation equipment a deployed, with capacity level $c^{'}$, during the strategic period $t^{'}$
$h_{ac't}$	Flow amount on arc a, with capacity level $c^{'}$, at the operational period t
g_{vct}	H_2 throughput amount at node v, with capacity level c, at the operational period t
s_{vct}	Amount of stored H_2 at storage node v, with capacity level c, at the operational period t

Parameters

$k^{CapEx}_{v,c,t'}, k^{CapEx}_{a,c',t'}$	Capital expenditures for the components of nodes/arcs with capacity level $c/c^{'}$ at strategic period $t^{'}$
$k^{OpEx}_{v,c,t}, k^{OpEx}_{a,c',t}$	Variable operating expenditures for the components of nodes/arcs with capacity level $c/c^{'}$ at operational period t
$k^{O\&M}_{v,c,t'}, k^{O\&M}_{a,c',t'}$	Fixed operation and maintenance expenditures for the components of nodes/arcs with capacity level $c/c^{'}$ at strategical period $t^{'}$
λ_v, λ_a	The percentage of H_2 that remains unlost after being processed at the nodes/transported along the arcs respectively. $\lambda_a \colon A \to [0,1]$ and $\lambda_v \colon V \to [0,1]$
$b_{v,c}, b_{a,c'}$	Operational capacity for the components of nodes/arcs for the capacity levels $c/c^{'}$ at the strategic period $t^{'}$ respectively
$d^{node}_{v,t}$	Demand amount for airports $v \in D$ at operational period t
ϕ_v, ϕ_a	Annuity cost factor for the components of nodes and arcs respectively, used to calculate the corresponding yearly capital expenditure.
μ	Weighted average capital cost (WACC)
$\alpha^{debt}, \alpha^{equity}$	Denote the debt and equity shares respectively over the initial capital expenditure
$\rho^{debt}, \rho^{equity}$	Annual rates of return on debt and equity respectively
ω	Corporate tax rate
γ	Depreciation time
β	Required LH_2 buffer stock at the airport (as a percentage of demand)
t_{max}	The corresponding number for the last operational time period
n	Number of operational periods per strategic period

3.1.3 Model formulation

The problem can be modeled as a mixed integer linear program as follows.

$$(3) \quad \min_{x,y,h,g,s} C(x,y,h,g,s)$$

$$\text{where } C(x,y,h,g,s) = \sum_{v\in V}\sum_{c\in C_v}\sum_{t'\in T'} k^{CapEx}_{v,c,t'} \cdot x_{v,c,t'} \cdot \phi_v \cdot \frac{t_{max} - (t'-1)\cdot n}{12}$$

$$+ \sum_{a\in A}\sum_{c'\in C_a}\sum_{t'\in T'} k^{CapEx}_{a,c',t'} \cdot y_{a,c',t'} \cdot \phi_a \cdot \frac{t_{max} - (t'-1)\cdot n}{12}$$

$$+ \sum_{v\in V}\sum_{c\in C_v}\sum_{t\in T} k^{OpEx}_{v,c,t} \cdot g_{v,c,t} + \sum_{a\in A}\sum_{c'\in C_a}\sum_{t\in T} k^{OpEx}_{a,c',t} \cdot h_{a,c',t}$$

$$+ \sum_{v\in V}\sum_{c\in C_v}\sum_{t'\in T'} k^{\text{O\&M}}_{v,c,t'} \cdot \left(\sum_{\tau\in T' :\, \tau\le t'} x_{v,c,\tau}\right) + \sum_{a\in A}\sum_{c'\in C_a}\sum_{t'\in T'} k^{\text{O\&M}}_{a,c',t'} \cdot \left(\sum_{\tau\in T' :\, \tau\le t'} y_{a,c',\tau}\right)$$

Regarding Equation (3), the linear function $C(x,y,h,g,s)$ serves as the objective function of the model, where the terms represent; total capital expenditures for nodes and arcs, total operating expenditures for nodes and arcs, and total fixed operation and maintenance expenditures for nodes and arcs, respectively. In addition to the total network cost, we incorporate refueling costs, which are calculated separately from the mathematical model (see Section 3.2).

For the first two terms, multiplication by ACF (ϕ) is applied to calculate the corresponding share of the total capital expenditures for the active periods in the modeling period. Similarly, last two terms, ensures to sum operation and maintenance expenditures for the nodes and arcs in their active years. The model minimizes the sum of these terms, yielding the total network expenditures.

$$(4.a) \quad \sum_{a\in\delta^+(v)}\sum_{c'\in C_a} \lambda_a \cdot h_{a,c',t} = d_{v,t} \qquad \forall v\in D, t\in T$$

$$(4.b) \quad \sum_{a\in\delta^+(v)}\sum_{c'\in C_a} \lambda_a \cdot h_{a,c',t} = \sum_{c\in C_v} g_{v,c,t} \qquad \forall v\in L\cup J\cup W,\ t\in T$$

$$(4.c) \quad \sum_{a\in\delta^-(v)}\sum_{c'\in C_a} h_{a,c',t} = \sum_{c\in C_v} \lambda_v \cdot g_{v,c,t} \qquad \forall v\in L\cup J\cup S\cup W_l,\ t\in T$$

$$(4.d) \quad \sum_{a\in\delta^+(v)}\sum_{c'\in C_a} \lambda_a \cdot h_{a,c',t} + \sum_{c\in C_v} \lambda_v \cdot s_{v,c,t-1} = \sum_{a\in\delta^-(v)}\sum_{c'\in C_a} h_{a,c',t} + \sum_{c\in C_v} s_{v,c,t} \qquad \forall v\in W_g, t\in T$$

The model accounts for losses in flow that occur both during transportation along arcs and during processing at nodes. The proportion of flow that remains, referred to as the "unlost" percentage, is characterized by the parameters $\lambda_a\colon A\to[0,1]$ for arcs and $\lambda_v\colon V\to[0,1]$ for nodes, respectively. The demand at each node is denoted by $d_{v,t}\colon (V,T)\to\mathbb{R}$. To ensure the proper allocation and conservation of flow throughout the network, the following constraints are imposed. Equation (4.a) ensures that the demand at each airport node is satisfied. Equation (4.b) equates the total incoming flow into a node, adjusted for losses along the incoming arcs, to the total throughput within the node. Conversely, Equation (4.c) balances the total outgoing flow from a node with the throughput, adjusted for losses occurring at the node itself. Due to the unique characteristics and requirements of different node types, Equations (4.b) and (4.c) are applied to distinct subsets of nodes. Together, these equations ensure flow conservation throughout the network, preventing the creation or disappearance of flow during transportation and processing. Since GH_2 can be stored for future use to optimize economic and capacity considerations, Equation (4.d) manages the flow-storage balance at GH_2 storage nodes. This equation guarantees that, across capacity levels, the cumulative incoming flow combined with the storage from the previous period matches the cumulative outgoing flow and the current storage amount.

$$(5.a)\quad g_{v,c,t} \leq \sum_{\substack{t' \in T' \\ n \cdot t' \geq t}} b^{node}_{v,c} \cdot x_{v,c,t'} \qquad \forall v \in L, c \in C_v, t \in T$$

$$(5.b)\ h_{a,c',t} \leq \sum_{\substack{t' \in T' \\ n \cdot t' \geq t}} b^{arc}_{a,c'} \cdot y_{a,c',t'} \qquad \forall a \in A, c^{'} \in C_a, t \in T$$

$$(5.c)\ g_{v,c,t} \leq\ b^{node}_{v,c} \cdot x_{v,c,t'} \qquad \forall v \in S, c \in C_v, t \in T, t^{'} \in T', t \leq n \cdot t'$$

$$(5.d)\ s_{v,c,t} \leq b^{node}_{v,c} \cdot x_{v,c,t'} \qquad \forall v \in W_g, t \in T, t^{'} \in T^{'}, t \leq n \cdot t'$$

$$(5.e)\quad g_{v,c,t} \cdot \frac{\beta}{\lambda_v} \leq \sum_{\substack{t' \in T' \\ n \cdot t' \geq t}} \sum_{c \in C_v} b^{node}_{v,c} \cdot x_{v,c,t'} \qquad \forall v \in W_l, t \in T, t^{'} \in T'$$

Equation (5.a) imposes a constraint such that the throughput at the liquefaction nodes cannot exceed the cumulated capacity of the node at the specified capacity level. Likewise, Equation (5.b) ensures that the flow on an arc does not exceed the cumulated capacity of the arc at the specified capacity level. Equations (5.c) and (5.d) also apply capacity limitations for supplier and gas storage nodes without cumulative capacity accounting, as these nodes are considered ready-to-use facilities with given capacities. Namely, the decisions regarding their utilization are made independently at the beginning of each strategic period and valid only in the specified strategic period. In addition to these capacity constraints, we assume that LH_2 storage includes a deterministic buffer size that is proportional to the demand of the airport which is stated in Equation (5.e). Since all LH_2 must pass through the LH_2 storage tank before refueling the aircraft, the airport demand equals the total incoming flow into the storage tanks, adjusted for losses at the tanks.

$$(6)\ y_{a,c',t'} =\ y_{a^R,c',t'} \qquad \forall a \in A, c^{'} \in C_a, t^{'} \in T^{'} \text{where } \exists a^R \in A$$

Certain arcs in the network can facilitate bidirectional flow. For instance, GH_2 can be transported in both directions between underground GH_2 storage nodes and their corresponding junction points. This bidirectional transmission is assumed to occur through the same pipeline but at different times. Consequently, arcs $a = (v, v', m)$ and $a^R = (v', v, m)$, which connect the same pair of nodes and enable flow in opposite directions, must be identical. This relationship is enforced by Equation (6).

$$(7)\ s_{v,c,t} = 0 \qquad \forall v \in W, c \in C_v, t = 0$$

$$(8.a)\ s_{v,c,t} \in \mathbb{R}_{\geq 0} \qquad \forall v \in W, c \in C_v, t \in T$$

$$(8.b)\ g_{v,c,t},\ h_{a,c',t} \in \mathbb{R}_{\geq 0} \qquad \forall v \in V, a \in A, c \in C_v, c^{'} \in C_a, t \in T$$

$$(8.c)\ x_{v,c,t'},\ y_{a,c',t'} \in\ \mathbb{Z}_{\geq 0} \qquad \forall a \in A, m \neq \text{"existing pipe"}, v \in L \cup W_l, c \in C_v, c^{'} \in C_a, t^{'} \in T'$$

$$(8.d)\ x_{v,c,t'},\ y_{a,c',t'} \in\ \{0, 1\} \qquad \forall a \in A, m = \text{"existing pipe"}, v \in S \cup W_g \cup D \cup J, c \in C_v, c^{'} \in C_a, t^{'} \in T'$$

Equation (7) initializes the stock level to zero. Equations (8.a) through (8.d) define the signs and types of the decision variables, ensuring consistency and feasibility in the solution space.

3.2 Approach for refueling at the airport and calculations

In this section, we discuss the chosen approach for modelling the LH_2 refueling at the airport and show the model equations. There are two different options for refuelling H_2 aircraft in the literature, analogous to conventional jet fuel refueling. One involves refuelling LH_2 directly with LH_2 refuelling trucks and the other involves using an LH_2 pipeline from which the aircraft can then be refuelled with the help of dispenser trucks. Hoelzen et

al. [1] compared both systems and found that hydrant refueling becomes economically favorable at annual LH_2 demands exceeding 125 kt H_2/a. However, additional factors such as traffic avoidance at space-constrained airports may influence the choice of refueling system. Given that the projected LH_2 demands at airports during the analyzed period remain well below this threshold, this study assumes refueling exclusively via LH_2 trucks. Since refueling costs primarily depend on demand and do not involve any decision variables influencing the network design, they do not affect the supply network optimization. Therefore, we handle refueling costs separately from the mathematical model and add them to the total network cost as an additional post-optimization component. In the following, the model equations are shown and explained. The total periodic cost of the refuelling $k^{TPC}_{ref,t'}$ in strategic period $t^{'}$ is calculated with;

$$k^{TPC}_{ref,t'} = k^{TPC,CapEx}_{i,t'} + k^{TPC,OpEx}_{i,t'} \quad (9)$$

where $k^{TPC,CapEx}_{i,t'}$ are the investment costs and $k^{TPC,OpEx}_{i,t'}$ the operational expenses of all components i in period $t^{'}$.

$$k^{TPC,CapEx}_{i,t'} = k^{TOT,CapEx}_{i,t'} \cdot \phi_i \quad (10)$$

$$k^{TPC,OpEx}_{i,t'} = k^{O\&M}_{i,t'} + k^{purging}_{t'} + k^{driver}_{t'} + k^{fuel}_{t'} \quad (11)$$

The total CapEx $k^{TOT,CapEx}_{i,t'}$ are calculated with Equation 11 with the number of refuelling truck $N_{reftruck,t'}$, the specific costs for the refueling truck $k^{CapEx}_{reftruck,t'}$, the specific cryo-pump costs $k^{CapEx}_{cryopump,t'}$ and maximum flow rate of the cryo-pump $\dot{m}_{reftruck}$. The cryo-pump is sized to 10 tLH_2/h in order to reach refueling times of around 15 min for a medium range H_2-powered aircraft with an LH_2 tank size of 2.5 tLH_2 (Schenke et al. 2025). The number of refueling trucks is determined by the maximum flow rate of the cryo-pump $\dot{m}_{reftruck}$, the availability factor of the refueling truck $f_{avail,reftruck}$ and the peak demand $\dot{m}_{H_2demand,t'}$ in Equation 12.

The operational expenses are calculated with the fixed operation and maintenance costs factor $k^{O\&M}_{i,t'}$, the costs for purging $k^{purging}_{t'}$, the driver costs $k^{driver}_{t'}$ and fuel costs $k^{fuel}_{t'}$ in Equation 11.

$$\dot{m}_{H_2demand,t'} \leq N_{reftruck,t'} \cdot \dot{m}_{reftruck} \cdot f_{avail,reftruck} \quad (12)$$

$$k^{TOT,CapEx}_{i,t'} = N_{reftruck,t'} \cdot (k^{CapEx}_{reftruck,t'} + k^{CAPEX}_{cryopump,t'} \cdot \dot{m}_{reftruck}) \quad (13)$$

$$k_{purging,t'} = m_{purgegas} \cdot N_{refevents,t'} \cdot k_{purgegas,t'} \quad (14)$$

$$N_{refevents,t'} = m_{H_2demand,y} \cdot \frac{1}{m_{aircrafttank}} \quad (15)$$

$$k^{TOT}_{driver,t'} = \theta_{reftruck,operation} \cdot f_{avail,reftruck} \cdot c_{driver,t'} \quad (16)$$

$$k^{TOT}_{fuel,t'} = N_{refevents,t'} \cdot \delta_{ref} \cdot m_{consumption,reftruck} \cdot k_{fuel,t'} \quad (17)$$

The purging costs are calculated with the number of refueling events $N_{refevents,t'}$ and the required amount of purge gas per refueling $m_{purgegas}$ and the specific costs for purge gas $k_{purgegas,t'}$. For more detailed information on the purge process it is referred to Mangold et al. (2022). The number of refueling events is calculated with the total H_2 demand and the specified size of an aircraft tank $m_{aircrafttank}$. The driver costs are calculated with the availability factor, the operation time of the refueling truck $\theta_{reftruck,operation}$ and the specific loan costs $c_{driver,t'}$. The fuel costs are calculated with the number of refueling events, the mean distance of one 3 km per refueling event δ_{ref}, the specific H_2 fuel consumption $m_{consumption,reftruck}$ of the fuel-cell powered refueling truck with the specific fuel costs $k_{fuel,t'}$.

4 Case study setting, data description and assumptions

To demonstrate the applicability of our model, we use it to analyze a case study on the future H_2 supply networks for airports in Germany. The case study comprises two demand scenarios. While the base scenario assumes market entry of H_2-powered aircraft in 2040 and reflects a conservative projection of H_2 demand, the moonshot scenario assumes market entry of H_2-powered aircraft in 2035 and adopts an optimistic demand outlook. The base scenario covers a planning horizon from 2041 to 2050 (due to negligible demand in 2040 and before), and the moonshot scenario already starts in 2036. These periods, analyzed at a monthly temporal resolution, provide a representative timeline, capturing the progression of H_2 utilization in aviation from its initial implementation to maturity. Operational decisions, such as flow and storage amounts, are analyzed at a monthly resolution, while strategic decisions, such as investing in facilities and transportation infrastructure, are assumed to be made every 5 years. This distinction reflects the long-term nature of strategic decisions,

which cannot be frequently adjusted and may, in practice, be reinforced by binding contracts or infrastructure commitments that ensure stability over extended periods.

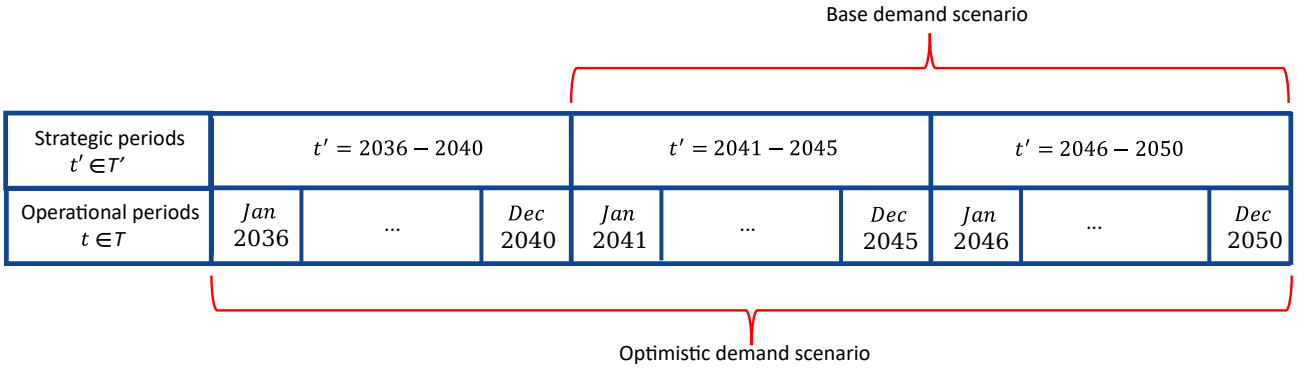

Fig. 5: Active periods in the case studies under base and optimistic demand scenarios

The scope of this research comprises nine representative airports in Germany. These airports account for approximately 85% of the nation's air traffic in terms of passengers numbers 2024 (ADV 2025), represent a range of sizes (small, medium, large), and are geographically well distributed across Germany, ensuring a comprehensive analysis. The selected airports with IATA codes are Berlin (BER), Bremen (BRE), Dresden (DRS), Dusseldorf (DUS), Frankfurt (FRA), Hamburg (HAM), Hannover (HAJ), Munich (MUC) and Stuttgart (STR). H2 demand at these airports is forecasted on a monthly basis. Aggregate demand across airports can be found in Figure 6.

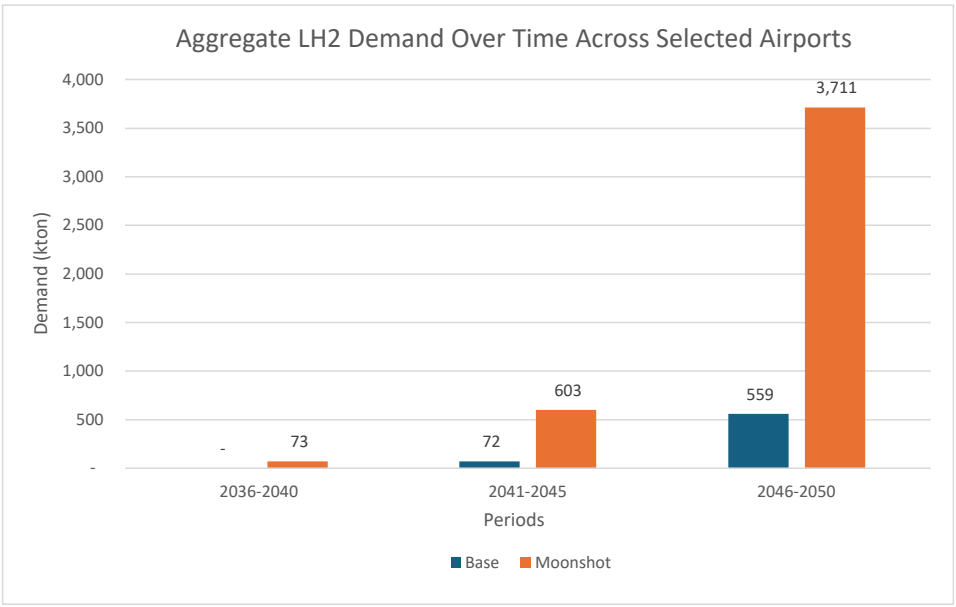

Fig. 6: Aggregate demand data for different periods and scenarios

To identify potential hydrogen suppliers, monthly production cost data for gaseous GH_2 across European regions, reported at the NUTS-1 level for 20,000 tons monthly production capacity, are utilized. These data accounts for regional variations in renewable energy resources and power grid infrastructures, which influence the cost of electricity generation and, consequently, the cost of GH_2 production. We selected 13 NUTS-1 production locations, including 6 as local production regions hosting the selected airports that are Saxony (DED), North

Rhine Westphalia (DEA), Hesse (DE7), Lower Saxony (DE9), Bavaria (DE2), Baden Wurttemberg (DE1). Although BER, HAM and BRE airports are located in Berlin (DE3), Hamburg (DE6), and Bremen (DE5) regions respectively, these three small regions are excluded due to their high residential area intensity and energy density, which result in insufficient available space for renewable electricity production to meet the hydrogen demand within the region. Additionally, we selected seven further lowest-cost regions in Europe — Denmark (DK0), Ireland (IE0), Norway (NO0), Central Spain (ES4), Finland (FI1), Czechia (CZ0), and Lithuania (LT0) — to analyze both regional and Europe-wide supply options. These regions, defined at the NUTS-1 level, are simplified to their geographic centers for modeling purposes. Furthermore, GH_2 production costs are calculated for monthly 20,000 tons production capacities, where the total production capacities of the hubs are validated to ensure they sufficiently meet the aggregate hydrogen demand of the selected airports, enabling a well-balanced and feasible solution. Although production costs varied with different production capacities, we observed stable price levels and consistent production feasibility across regions at a capacity of 20,000 tons. Both the demand and GH_2 production cost datasets were provided by the different workpackages of the HyNEAT project , of which this study is a component. Additionally, European Hydrogen Backbone (EHB) projections for underground hydrogen storage infrastructure were integrated into our dataset as existing GH_2 storage facilities, commissioned according to their projected timelines. They are designated to store excess H_2 production from the nearest production hub and 12 of them (the closest ones to 13 production hubs) are included. Detailed case study network is presented in Figure 8(a).

For the network design, we incorporated projections from the EHB for existing pipeline infrastructure. Specifically, the EHB's pipeline scenarios for 2030 and 2040 were used to represent the infrastructure for the periods 2036–2039 and 2040–2050, respectively. This infrastructure dynamically evolves within our dataset to reflect its status during each strategical time period of the study. Junction nodes were added to the dataset to connect the closest points of production hubs, airports, and storage facilities to the pipeline infrastructure. It is assumed that connections to the existing pipeline infrastructure can be established at any point along its route. The geographical data for EHB pipelines and underground storage facilities, as well as the identification of junction nodes, were obtained and analyzed using QGIS (Quantum Geographic Information System) software. Given the infeasibility of transporting LH_2 over long distances via pipelines and the economic disadvantages of using trucks for GH_2 transport, we assumed the use of EHB (existing) and newly installed pipelines for GH_2 and trucks for LH_2 transportation within the specified network. EHB tariff structures were applied to account for using existing infrastructures. The tariff rates represent flow-dependent service fees and can be considered as OpEx. However, they inherently incorporate the CapEx; therefore, no separate or explicit CapEx component is accounted for the use of EHB's projected backbone. Besides, other techno-economic parameters for the network components, including CapEx and OpEx, are based on Hoelzen et al. (2023) and HyNEAT internal data (see Supplementary Information A.1). These parameters are calculated for different time periods and capacity levels, capturing economies of scale in an inflation-free environment. A buffer stock equivalent to three days of airport hydrogen demand is assumed to be maintained in the LH_2 storage tanks. Lastly, the parameters used in ACF calculations are presented in Supplementary Information A.1.

The optimization model was implemented in Python 3.12 and solved using Gurobi 12.0.0 on a Windows notebook with 2.1 GHz CPU (12 cores) and 16 GB RAM. We set a time limit of 6 hours for each run. For the base demand scenario, covering the 10-year period from 2041 to 2050, the model reached optimality in 4 hours and 32 minutes. For the moonshot scenario, which spans 15 years (2036–2050), a 0.83% optimality gap was achieved within the 6-hour time limit.

5 Results and discussion

According to the optimal network design results (see Figure 7), the average LH_2 supply cost across the entire network is estimated at 6.07 USD/kgLH_2 and 3.28 USD/kgLH_2 for the base demand scenario in the periods 2041–2045 and 2046–2050, respectively. For the moonshot scenario, the costs are estimated at 6.62 USD/kgLH_2, 3.87 USD/kgLH_2, and 3.06 USD/kgLH_2 for the periods 2036–2040, 2041–2045, and 2046–2050, respectively. This reflects a cost reduction of more than 50% over ten years in the moonshot scenario and approximately 45% over five years in the base scenario. The primary driver of this cost decline is the decreasing price of green electricity, which directly reduces the cost of GH_2 production and liquefaction. Additionally, the growing scale of hydrogen utilization enables the system to benefit from economies of scale, as well as improved utility and efficiency in liquefaction, storage, transportation, and refueling processes. A significant portion of the total cost, ranging between 75% and 90%, is attributed to two main components: GH_2 production and liquefaction. Transportation also plays a considerable role in earlier periods, accounting for more than 20% of the cost. However, with increasing demand and a transition from truck-based to pipeline-based transport (see Figure 9), this share drops to around 10%. Under the case study assumptions, which include a three-day LH_2 storage

buffer at airports, LH_2 storage costs contribute approximately 1–3% to the total cost, while GH_2 storage has no role in that.

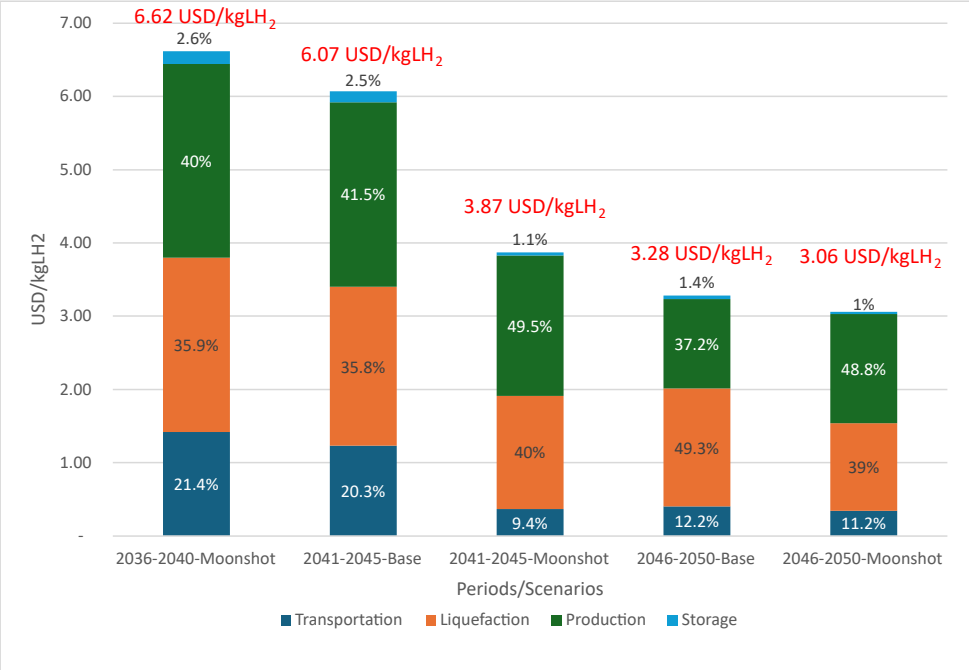

Fig. 7: Average total network cost and shares for different categories over the modeling periods and demand scenarios

The moonshot scenario is not an exact match but can be seen as a roughly five-year-forward projection of the base scenario in terms of demand levels. Therefore, despite the differences in electricity and material costs across time periods, we observed notable similarities between the results of the earlier strategic phases of the moonshot scenario and the subsequent phases of the base scenario. All detailed results for both scenarios are provided in Supplementary Information A.2. However, to maintain clarity and focus, and to present a longer modeling horizon, we focus exclusively on the moonshot scenario in the remainder of this chapter.

In Figure 8(a), the case study network is presented, while Figures 8(b)–(d) show the optimal network layouts for the respective time periods. We observe that over time, as demand increases, new production hubs become active. In other words, the number of operational production hubs grows, and each airport increasingly receives supply from multiple production hubs. One reason for this is that, due to production capacity limits, new suppliers must be activated to meet the increasing demand. Another contributing factor is that, while truck transportation is initially preferred when demand is low, it becomes economically less favorable as demand rises. Consequently, pipeline transport replaces trucks, making it feasible to supply airports from more distant production hubs. For example, during the 2036–2040 strategic period, nearby production hubs and Ireland (due to its cost advantages) are primarily preferred. However, in later periods, we observe supply connections also emerging from more distant locations such as Finland and Spain. As expected, these dynamics lead to increased network complexity over time, driven by the rising demand.

Differing climate conditions across regions influence the production costs of green electricity, and consequently, the cost of hydrogen. As a result, we observe that airports are supplied by multiple production hubs (besides capacity and transportation mode factors) to ensure access to the cheapest available hydrogen. This multi-sourcing strategy allows airports to benefit from cost advantages offered by different production hubs across seasons. For example, in the year 2050, Munich Airport is primarily supplied by Lithuania, Denmark, and Finland during the winter and early spring months (January, February, March, November, December) where the wind is a main renewable energy source, whereas during the warmer months (April to October), its supply mainly comes from Central Spain, Saxony, and Czechia where solar energy plays an important role. This also leads to the avoidance of underground storage, as producing excess hydrogen during low-cost periods and storing it for future use turns out to be less favorable option than diversifying suppliers. Therefore, the results suggest that there is no need for underground storage.

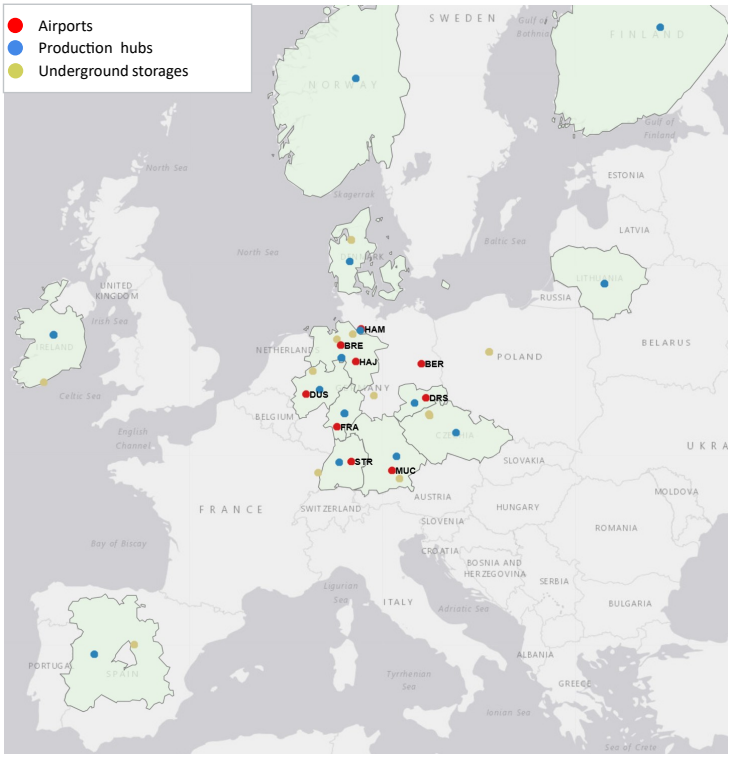

(a) Case study network

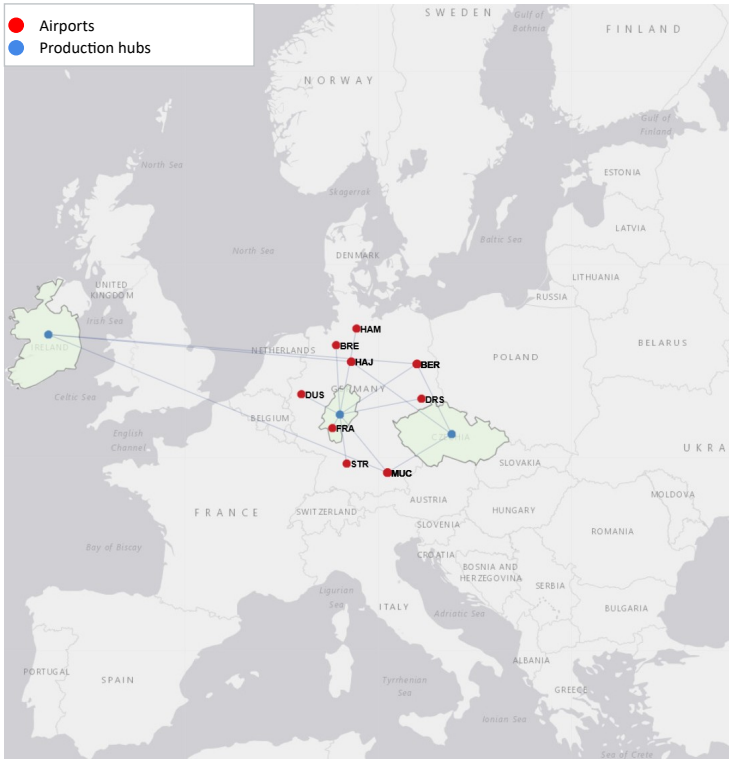

(b) Optimal network (2036–2040)

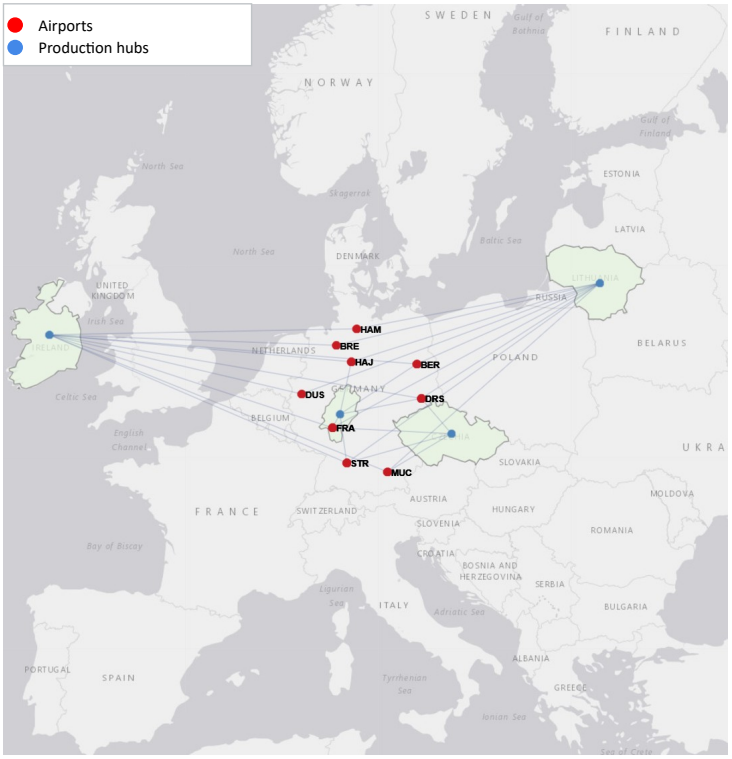

(c) Optimal network (2041–2045)

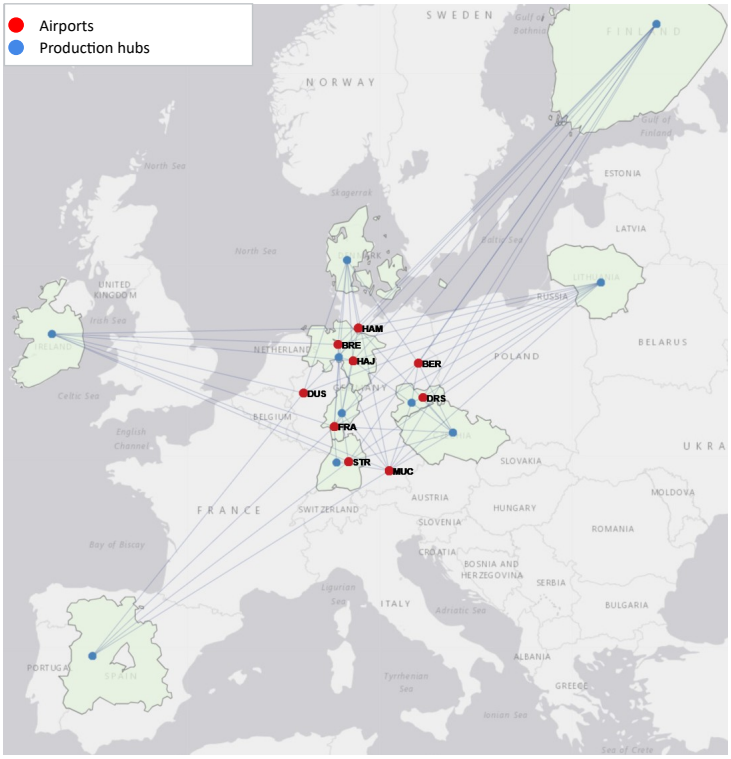

(d) Optimal network (2046–2050)

Fig. 8: Case study and optimal network maps

As mentioned previously in this section, the use of trucks decreases over time as demand increases, while the share of existing pipelines (i.e. projected EHB pipelines) rises. The reason pipelines are not utilized extensively in the first strategic period is that there are still upfront investments required to connect existing pipelines to both the airports and the production hubs. These investments become economically favorable only when the scale of operations justifies them. After the first period, the majority of hydrogen is transported via the existing pipelines. The shares of the transportation modes are shown in Figure 9. Additionally, despite the high costs, we observe the installation of new pipelines supplying Frankfurt and Stuttgart from their respective regions, Hesse and Baden-Wurttemberg. This indicates that, under certain conditions—namely, when the distance is not excessive, the demand is at sufficient scale, and no suitable existing pipeline infrastructure is available—new pipelines may be preferred over trucks, even despite the substantial investments. All details regarding the transportation modes employed between production hubs and airports are provided in Supplementary Information A.2.

Transportation mode/periods	2036-2040	2041-2045	2046-2050
Existing Pipeline (EHB)	22%	97%	89%
New Pipeline	-	-	8%
Truck	78%	3%	3%

Fig. 9: Share of transportation modes used for transportation H_2

When we examine the costs at each individual airport, we also observe a steep reduction in costs over the analyzed periods. Furthermore, we find that the supply cost is strongly inversely correlated with the airport's demand. For the period 2046–2050, the average network cost was 3.06 USD/kg_{LH_2}, as stated earlier. Airports with the four highest demands—Frankfurt, Munich, Berlin, and Dusseldorf—have lower supply costs than the network average. Conversely, smaller airports such as Hannover and Dresden face higher LH_2 supply costs. Interestingly, although Bremen is a relatively small airport, it benefits from notably low supply costs due to its direct connection to the existing pipeline backbone and the low regional electricity prices, which lead to reduced liquefaction costs at the airport. Similar to supply cost, we observe also steep reduction in refueling costs. In the first period, the low demand leads to inefficient utilization of refueling trucks, resulting in exceptionally high refueling costs that sometimes exceeding the supply cost at smaller airports such as Dresden. In contrast, by the final period, refueling costs decrease significantly, accounting for approximately 5–15% of the supply cost. Figure 10 presents the LH_2 supply costs and refueling costs at each airport.

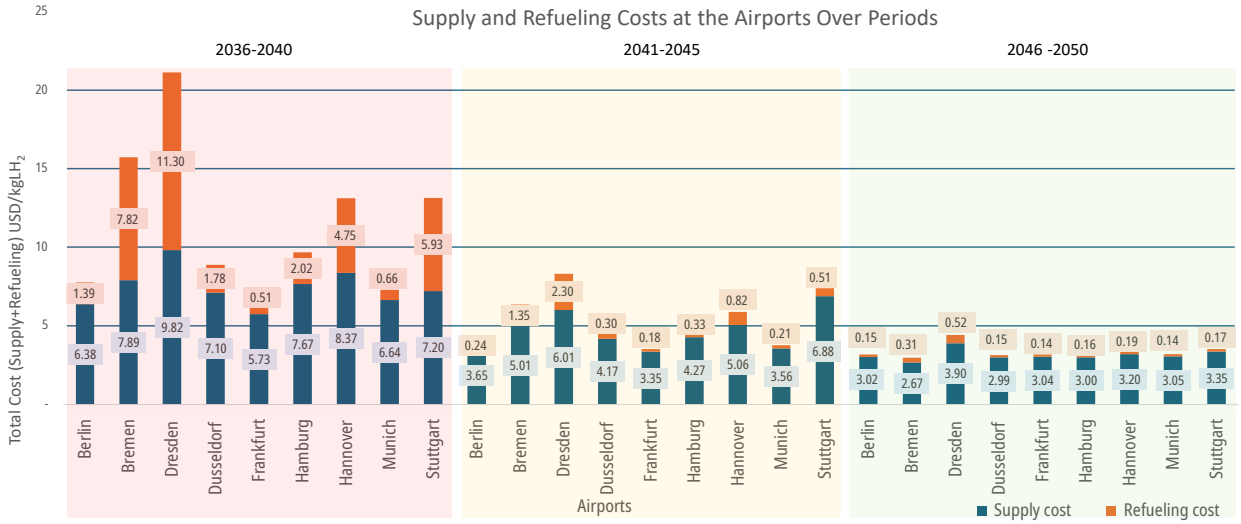

Fig. 10: LH_2 supply and refueling costs at the airports over the modeling periods (USD/$kgLH_2$)

6 Conclusion and outlook

This study involves the development of a multi-period mathematical model for the cost-optimal HSCND. The model accounts for key requirements such as economies of scale, different transportation modes, the handling of various hydrogen phases, and hydrogen losses. Rather than focusing solely on the construction of new infrastructure, it also considers future underground storage and pipeline infrastructures, providing a more realistic approach. In addition, the model incorporates a monthly temporal resolution to carefully capture trends in demand and GH_2 production costs over time. Based on these requirements, the model provides an analytical decision support mechanism regarding facility capacities, supply locations, storage quantities, and transportation modes.

When tested on a case study, the model revealed several important insights. First, while truck transportation is advantageous in the early years at small scales, the model indicates that, at larger scales, existing pipelines will play a major role in transporting hydrogen for aviation in the future. Therefore, the projected infrastructure plans, such as those proposed by the EHB, are crucial for ensuring the cost advantage of hydrogen. Moreover, thanks to the existing pipelines, it will be possible to source from distant but more cost-efficient production hubs. For this reason, if the hydrogen economy is to materialize, retrofitting natural gas pipelines into hydrogen pipelines will be a critical prerequisite. To make such retrofitting meaningful and effective, however, not only the aviation sector but also several other sectors will need to use hydrogen, ensuring that the retrofitted pipelines operate at high utilization rates. Thus, the creation of a broad hydrogen ecosystem with cross-sectoral demand is another key prerequisite.

According to the model results, no underground storage was employed. The reason for this is that airports can flexibly source from multiple production hubs located in regions with varying climate characteristics across different months. While the model does not impose restrictions on supplier diversification, it is worth noting that, in real life, long-term contracts and purchase guarantees may arise. In such cases, hydrogen storage may become important. More importantly, from an energy security perspective, underground storage as a national buffer stock is one of the most critical instruments. Therefore, even though the model does not recommend underground storage under the current assumptions, infrastructure investments for underground storage should not be neglected due to such real-world constraints and requirements.

In our case study, production hubs with low costs across Europe were considered, with their production capacities capped at 20,000 tons, and the corresponding hydrogen costs were taken into account. Under this capacity and the number of available production hubs, no issue arose regarding demand satisfaction. However, if hydrogen demand cannot be fully met in the future, competition may emerge between sectors to access the cheapest hydrogen sources. To ensure fairness in such competition, issues like hydrogen market regulations should be part of the political agenda. Furthermore, for energy security, infrastructure investments and supply agreements with suppliers in diverse locations such as Chile, Namibia, and Morocco should start as soon as possible.

While the results of our model are promising, there are several areas where this study could be further expanded. For example, a broader and more holistic approach could be considered by integrating sustainable aviation fuels (SAFs) alongside hydrogen, redesigning the network accordingly. On the other hand, the cost-oriented objective function can be extended to include ecological and social objectives within a multi-objective framework, enabling a more comprehensive sustainable supply chain design.

Declaration of generative AI and AI-assisted technologies in the writing process: During the preparation of this work the authors used DeepL and ChatGPT in order to improve grammer and enhance clarity. After using this tool/service, the authors reviewed and edited the content as needed and take full responsibility for the content of the publication.

Bibliography

[1] Airbus (2025). Advancing alternative-propulsion technology, https://www.airbus.com/en/innovation/low-carbon-aviation/hydrogen. Last accessed 30 January 2025

[2] Ajanovic, A., Sayer, M., Haas, R. (2022). The economics and the environmental benignity of different colors of hydrogen, International Journal of Hydrogen Energy, 47(57), 24136-24154. https://doi.org/10.1016/j.ijhydene.2022.02.094.

[3] Almansoori, A., and Shah, N. (2009). Design and operation of a future hydrogen supply chain: Multi-period model. International Journal of Hydrogen Energy, 34(19), 7883–7897. https://doi.org/10.1016/j.ijhydene.2009.07.109

[4] Almansoori, A., and Shah, N. (2012). Design and operation of a stochastic hydrogen supply chain network under demand uncertainty. International Journal of Hydrogen Energy, 37(5), 3965–3977. https://doi.org/10.1016/j.ijhydene.2011.11.091

[5] Almansoori, A., Betancourt-Torcat, A. (2016). Design of optimization model for a hydrogen supply chain under emission constraints - A case study of Germany. Energy **2**(111), 414–429 https://doi.org/10.1016/j.energy.2016.05.123

[6] Baufumé, S., Grüger, F., Grube, T., Krieg, D., Linssen, J., Weber, M., Hake, J.-F., and Stolten, D. (2013). GIS-based scenario calculations for a nationwide German hydrogen pipeline infrastructure. International Journal of Hydrogen Energy, 38(10), 3813–3829. https://doi.org/10.1016/j.ijhydene.2012.12.147

[7] Cerniauskas, S., Jose Chavez Junco, A., Grube, T., Robinius, M., and Stolten, D. (2020). Options of natural gas pipeline reassignment for hydrogen: Cost assessment for a Germany case study. International Journal of Hydrogen Energy, 45(21), 12095–12107. https://doi.org/10.1016/j.ijhydene.2020.02.121

[8] De-León Almaraz, S., Azzaro-Pantel, C., Montastruc, L., and Domenech, S. (2014). Hydrogen supply chain optimization for deployment scenarios in the Midi-Pyrénées region, France. International Journal of Hydrogen Energy, 39(23), 11831–11845. https://doi.org/10.1016/j.ijhydene.2014.05.165

[9] Erdoğan, A., and Güler, M. G. (2023). Optimization and analysis of a hydrogen supply chain in terms of cost, CO2 emissions, and risk: The case of Turkey. International Journal of Hydrogen Energy, 48(60), 22752–22765. https://doi.org/10.1016/j.ijhydene.2023.04.300

[10] Eskandari, M., Gilani, H., Sahebi, H., and Sharifi, S. (2024). Design and planning of global sustainable bio-hydrogen supply chain with uncertainty: A transportation-oriented robust model. Chemical Engineering Science, 283, 119365. https://doi.org/10.1016/j.ces.2023.119365

[11] European Hydrogen Backbone Initiative: Hydrogen Pipeline Backbone Maps, https://www.h2inframap.eu/#map. Last accessed 30 January 2025

[12] Fazli-Khalaf, M., Naderi, B., Mohammadi, M., Pishvaee, M.S. (2020). Design of a sustainable and reliable hydrogen supply chain network under mixed uncertainties: A case study. International Journal of Hydrogen Energy, 45, 59, 34503-34531,https://doi.org/10.1016/j.ijhydene.2020.05.276

[13] Flughafenverband ADV (2025). Monthly Traffic Report. https://www.adv.aero/wp-content/uploads/2015/11/12.2024-ADV-Monatsstatistik.pdf. Last accessed 30 January 2025

[14] Forghani, K., Kia, R., and Nejatbakhsh, Y. (2023). A multi-period sustainable hydrogen supply chain model considering pipeline routing and carbon emissions: The case study of Oman. Renewable and Sustainable Energy Reviews, 173, 113051. https://doi.org/10.1016/j.rser.2022.113051

[15] Goetschalckx, M. (2011). Supply Chain Engineering. International series in operations research and management science. https://doi.org/10.1007/978-1-4419-6512-7

[16] Güler, M. G., Geçici, E., and Erdoğan, A. (2021). Design of a future hydrogen supply chain: A multi period model for Turkey. International Journal of Hydrogen Energy, 46(30), 16279–16298. https://doi.org/10.1016/j.ijhydene.2020.09.018

[17] Harrington, T.: "Airbus Delays Its Zeroe Hydrogen Aircraft as UK CAA Expands Hydrogen Programme." GreenAir News, 10 Feb. 2025, www.greenairnews.com/?p=6742. Last accessed 6 April 2025

[18] Hoelzen, J., Flohr, M., Silberhorn, D., Mangold, J., Bensmann, A., and Hanke-Rauschenbach, R. (2022). H2-powered aviation at airports – Design and economics of LH2 refueling systems. Energy Conversion and Management: X, 14, 100206. https://doi.org/10.1016/j.ecmx.2022.100206

[19] Hoelzen, J., Koenemann, L., Kistner, L., Schenke, F., Bensmann, A., and Hanke-Rauschenbach, R. (2023). H2-powered aviation – Design and economics of green LH2 supply for airports. Energy Conversion and Management: X, 20, 100442. https://doi.org/10.1016/j.ecmx.2023.100442

[20] Hydrogen Central, Aviation Could Use up to 20% of World's Hydrogen Supply by 2050 for Decarbonisation. https://hydrogen-central.com/aviation-couldworlds-hydrogen-supply-2050-decarbonisation-iata/. Last accessed 30 January 2025

[21] HyNeat Project Homepage, https://www.hyneat.de/. Last accessed 30 January 2025

[22] IATA (2025). Our Commitment to Fly Net Zero by 2050. iata.org/en/programs/environment/flynetzero/. Last accessed 30 January 2025

[23] International Energy Agency (IEA): Aviation. https://www.iea.org/energy-system/transport/aviation Last accessed 30 January 2025

[24] Kim, S., Park, J., Chung, W., Adams, D., and Lee, J. H. (2024). Techno-economic analysis for design and management of international green hydrogen supply chain under uncertainty: An integrated temporal planning approach. Energy Conversion and Management, 301, 118010. https://doi.org/10.1016/j.enconman.2023.118010

[25] Lahnaoui, A., Wulf, C., Dalmazzone, D. (2021). Optimization of hydrogen cost and transport technology in France and Germany for various production and demand scenarios. Energies **14**(3), 744. https://doi.org/10.3390/en14030744

[26] Lee, D. S., Fahey, D. W., Skowron, A., Allen, M. R., Burkhardt, U., Chen, Q., Doherty, S. J., Freeman, S., Forster, P. M., Fuglestvedt, J., Gettelman, A., De León, R. R., Lim, L. L., Lund, M. T., Millar, R. J., Owen, B., Penner, J. E., Pitari, G., Prather, M. J., ... Wilcox, L. J. (2021). The contribution of global aviation to anthropogenic climate forcing for 2000 to 2018. Atmospheric Environment, 244, 117834. https://doi.org/10.1016/j.atmosenv.2020.117834

[27] Mangold, J., Silberhorn, D., Moebs, N., Dzikus, N., Hoelzen, J., Zill, T., Strohmayer, A. (2022). Refueling of LH2 Aircraft—Assessment of Turnaround Procedures and Aircraft Design Implication. Energies, 15, 2475. https://doi.org/10.3390/en15072475.

[28] Fuel Cells and Hydrogen 2 Joint Undertaking. (2020). Hydrogen-powered aviation : a fact-based study of hydrogen technology, economics, and climate impact by 2050. Publications Office. https://data.europa.eu/doi/10.2843/471510.

[29] Melo, M.T., Nickel, S., Saldanha-da-Gama, F. (2009). Facility location and supply chain management – A review. European Journal of Operational Research,196, 401-412. https://doi.org/10.1016/j.ejor.2008.05.007.

[30] Moreno-Benito, M., Agnolucci, P., and Papageorgiou, L. G. (2017). Towards a sustainable hydrogen economy: Optimisation-based framework for hydrogen infrastructure development. Computers and Chemical Engineering, 102, 110–127. https://doi.org/10.1016/j.compchemeng.2016.08.005

[31] Mukherjee, U., Elsholkami, M., Walker, S., Fowler, M., Elkamel, A., and Hajimiragha, A. (2015). Optimal sizing of an electrolytic hydrogen production system using an existing natural gas infrastructure. International Journal of Hydrogen Energy, 40(31), 9760–9772. https://doi.org/10.1016/j.ijhydene.2015.05.102

[32] Ochoa Bique, A., and Zondervan, E. (2018). An outlook towards hydrogen supply chain networks in 2050—Design of novel fuel infrastructures in Germany. Chemical Engineering Research and Design, 134, 90–103. https://doi.org/10.1016/j.cherd.2018.03.037

[33] Ohmstede, K., Thies, C., Barke, A., Spengler, T.S. (2023). Evaluation of Hydrogen Supply Options for Sustainable Aviation. In: Buscher, U., Neufeld, J.S., Lasch, R., Schönberger, J. (eds) Logistics Management. LM 2023. Lecture Notes in Logistics. Springer, Cham. https://doi.org/10.1007/978-3-031-38145

[34] Ögrük, A., Marx, R., Thies, C., Stiller, S. (2025). Green Hydrogen Supply Chain Network Design for Aviation: Model Development and Case Study for German Airports in 2050. In: Voigt, G., Fliedner, M., Haase, K., Brüggemann, W., Hoberg, K., Meissner, J. (eds) Operations Research Proceedings 2023. OR 2023. Lecture Notes in Operations Research. Springer, Cham. https://doi.org/10.1007/978-3-031-58405-3_58

[35] Raaesi, R., Searle, C., Balta-Ozkan, N., Marsiliani, L., Tian, M., and Greening, P. (2024). Hydrogen supply chain and refuelling network design: Assessment of alternative scenarios for the long-haul road freight in the UK. International Journal of Hydrogen Energy, 52, 667–687. https://doi.org/10.1016/j.ijhydene.2023.03.474

[36] Reuß, M., Grube, T., Robinius, M., Preuster, P., Wasserscheid, P., and Stolten, D. (2017). Seasonal storage and alternative carriers: A flexible hydrogen supply chain model. Applied Energy, 200, 290–302. https://doi.org/10.1016/j.apenergy.2017.05.050

[37] Reuß, M., Grube, T., Robinius, M., and Stolten, D. (2019). A hydrogen supply chain with spatial resolution: Comparative analysis of infrastructure technologies in Germany. Applied Energy, 247, 438–453. https://doi.org/10.1016/j.apenergy.2019.04.064

[38] Ochoa-Robles, J., Billoud, M.G., Azzaro-Pantel, C., Aguilar-Lasserre, A.A.(2019). Optimal Design of a Sustainable Hydrogen Supply Chain Network: Application in an Airport Ecosystem. ACS Sustainable Chemistry I& Engineering **7**(21), 17587. https://doi.org/10.1021/acssuschemeng.9b02620

[39] Rosalyne, M.: Successful test flight of hydrogen-powered plane gives sustainable aviation a lift. https://www.euronews.com/next/2023/03/13/successful-test-flight-of-hydrogen-powered-plane-gives-sustainable-aviation-a-lift. Last accessed 30 January 2025

[40] Schenke, F., Hoelzen, J., Bredemeier, D., Schomburg, L., Bensmann, A., Hanke-Rauschenbach, R. (2024). LH2 supply for the initial development phase of H2-powered aviation. Energy Conversion and Management: X, Volume 24, 2024, 100797,https://doi.org/10.1016/j.ecmx.2024.100797

[41] Schenke, F., Koenemann, L., Hoelzen, J., Schelm, ., Bensmann, A., and Hanke-Rauschenbach, R. (2025). Planning Lh2 Infrastructure for H2-Powered Aviation: From the Initial Development to Market Penetration. Available at SSRN: https://ssrn.com/abstract=5205289orhttp://dx.doi.org/10.2139/ssrn.5205289

[42] Sens, L., Piguel, Y., Neuling, U., Timmerberg, S., Wilbrand, K., and Kaltschmitt, M. (2022). Cost minimized hydrogen from solar and wind – Production and supply in the European catchment area. Energy Conversion and Management, 265, 115742. https://doi.org/10.1016/j.enconman.2022.115742

[43] Silva, F. B., Da Silva, C., and Barbosa-Póvoa, A. P. (2024). Design and planning green hydrogen supply chains: Characterization and optimization. In Computer Aided Chemical Engineering (Vol. 53, pp. 2419–2424). Elsevier. https://doi.org/10.1016/B978-0-443-28824-1.50404-X

[44] Sizaire, P., Lin, B., and Gençer, E. (2024). A novel hydrogen supply chain optimization model – Case study of Texas and Louisiana. International Journal of Hydrogen Energy, 78, 401–420. https://doi.org/10.1016/j.ijhydene.2024.06.236

[45] The Federal Government Website (2025). National Hydrogen Strategy. https://https://www.bundesregierung.de/breg-de/service/archiv-bundesregierung/hydrogen-technology-2204238. Last accessed 30 January 2025

[46] Uster, H., Dilaveroğlu, Ş. (2014). Optimization for design and operation of natural gas transmission networks. Applied Energy **133**, 56–69. https://doi.org/10.1016/j.apenergy.2014.06.042

[47] Wickham, D., Hawkes, A., Jalil-Vega, F. (2021). Hydrogen supply chain optimisation for the transport sector – Focus on hydrogen purity and purification requirements. Applied Energy, **305**,117740. https://doi.org/10.1016/j.apenergy.2021.117740

[48] Wolff, M., Becker, T., Walther, G. (2023). Long-term design and analysis of Renewable Fuel Supply Chains – an integrated approach considering seasonal resource availability. European Journal of Operational Research **304**(2),745–762. https://doi.org/10.1016/j.ejor.2022.04.001

[49] Yoon, H.J., Seo, S.K., and Lee, C.J. (2022). Multi-period optimization of hydrogen supply chain utilizing natural gas pipelines and byproduct hydrogen. Renewable and Sustainable Energy Reviews **157**,112083. https://doi.org/10.1016/j.rser.2022.112083